An angle-dependent potential and alpha-decay half-lives of deformed nuclei for $67\leqslant Z\leqslant 91$

H. Hassanabadi[1] E. Javadimanesh[1;1)] S. Zarrinkamar[2] H. Rahimov[3]

[1] Physics Department, Shahrood University of Technology, Shahrood, Iran
[2] Department of Basic Science, Garmsar Branch, Islamic Azad University, Garmsar, Iran
[3] Computer Engineering Department, Shahrood University of Technology, Shahrood, Iran

Abstract: The half-lives of deformed nuclei are reported for $67\leqslant Z\leqslant 91$. We consider an angle-dependent potential which yields multiple approximations. The results are in better agreement with the experimental data when the multiple approximation is solely considered for the daughter nuclei.

Key words: alpha decay, deformed nuclei, ground state, multiple approximation

PACS: 23.60.+e, 23.35.+g, 27.70.+q **DOI:** 10.1088/1674-1137/37/4/044101

1 Introduction

Alpha decay (AD) is one of the physical processes that can be successfully described in the introductory quantum theory. The underlying mechanism was first explained by Gamow [1], Gurney and Condon [2] in 1928 under the title of the quantum tunneling effect which can be chronologically considered as the first successful quantum description of nuclear phenomenon. There exists much notable work on the subject of AD and related topics. Xu and Ren reported the alpha decay half-lives (ADHL) within the density-dependent cluster model [3]. ADHL of heavy and super heavy nuclei were obtained using a radial wave function via the cluster model by Ni and Ren [4]. An analytical formula for log $(T_{1/2}(\mathrm{s}))$ based on a recent selected data set of partial ADHL of 344 ground- state (Gs) to Gs transitions was proposed by Royer [5]. The modified two-potential approach within the density-dependent cluster model was applied to the subject by Yibin and Ren [6]. Stone et al. worked on the results of low temperature nuclear orientation experiments to investigate the AD and the consequent half-lives (HL) [7]. Calculations on the ADHL of even-even medium mass nuclei within the density-dependent cluster model using a two-potential approach were performed by Yibin et al [8]. Barriers standing against the formation of super heavy elements and their consecutive AD in the quasimolecular shape path were studied within a generalized liquid drop model (GLDM) by Royer et al. [9]. The problem was analyzed by Tavares et al. via quantum mechanical tunneling through a potential barrier. They took into account the centrifugal and overlapping effects as well [10]. A semi-empirical model based on the quantum-mechanical tunneling mechanism of alpha emission was suggested by Medeiros et al. [11]. Spontaneous fission HL of heavy nuclei in ground and isomeric states was studied by Ren and Chang Xu [12]. Samanta et al. provided theoretical estimates for the HL of several isotopes of heavy elements by calculating the quantum mechanical tunneling probability in a WKB framework. In their calculations, they used the microscopic nucleus-nucleus potential obtained via folding the densities of interacting nuclei with the DDM3Y effective nuclear interaction [13]. A new semi-empirical formula for determining the spontaneous fission HL was introduced by the work of Santhosh et al. [14]. Many related concepts, including the predictabilities of the three ADHL, the Royer GLDM, the Viola-Seaborg and the Sobiczewski-Parkhomenko formulae were investigated by Dasgupta-Schuber et al. through developing a method based on standard experimental benchmarking [15]. The possible effect of the solid-state environment of the decaying nucleus on the HL was investigated in Refs. [16, 17].

As many alpha-emitters are deformed, considering an angle-dependent potential looks quite logical [18, 19]. In this article, contrary to other papers, we have calculated the HL of some deformed nuclei from Gs to Gs transitions. Our work is organized as follows. We first review the AD within the proximity approach. We next report our results for various modes and make a comparison with the existing experimental data and a previous paper.

Received 2 May 2012

1) E-mail: elham_javadimanesh89@yahpoo.com

2 The formalism of alpha decay in the proximity approach

Within the Coulomb and proximity potential model for deformed nuclei, the potential energy barrier is normally considered as a sum of the Coulomb, proximity and centrifugal potentials for the touching configuration and for the separated fragments. The potential $V(r)$ includes two parts in the over- lapping ($r<C_t$) and nonoverlapping ($r\geqslant C_t$) regions. We consider the potential as [20, 21]

$$V(r)=\begin{cases} a_0+a_1r+a_2r^2 & R_p\leqslant r<C_t. \\ V_c(r)+V_{prox}(z)+V_l(r) & r\geqslant C_t. \end{cases} \tag{1}$$

where $V_l(r)=\dfrac{\hbar^2 l(l+1)}{2\mu r^2}$ stands for the centrifugal potential where $\mu=m\dfrac{A_dA_\alpha}{A_d+A_\alpha}$ and m, A_d and A_α respectively denote the nucleon mass, mass number of daughter nuclei and Alpha particle. $V_{prox}(z)$ represents the proximity potential and z is the distance between the near surfaces of the fragments. The coulomb potential V_c between the deformed daughter and emitted alpha particle is given by $V_c(r)=\dfrac{Z_dZ_\alpha e^2}{r}$, with Z_d and Z_α being the atomic numbers of daughter and parent nuclei, respectively. In addition, $r=z+\overline{C}_d(\theta)+C_\alpha$ is the distance between the fragment centers with [22]

$$\overline{C}_t(\theta)=\overline{C}_d(\theta)+C_\alpha. \tag{2}$$

The Süssmann central radius $C_d(\theta)$ of the daughter is related to $R_d(\theta)$ via [23]

$$C_d(\theta)=R_d(\theta)-\frac{1}{2}kb^2, \tag{3}$$

where k is the total curvature of the surface at the point under consideration and $b\approx1$ represents the width of the nuclear surface. The Süssmann central radius C_α of the emitted Alpha is [23]

$$C_\alpha=R_\alpha-\frac{b^2}{R_\alpha}, \tag{4}$$

R_i are the sharp radii related to mass number A_i via [24]

$$R_i=1.28A_i^{1/3}-0.76+0.8A_i^{-1/3}. \tag{5}$$

where i=p, d, α respectively denote the parent, daughter and the Alpha. For deformed shape nuclei, we define [25]

$$R_i(\theta)=R_i\left[1+\sum_{n=0}^{\infty}\sqrt{\frac{2l+1}{4\pi}}\beta_lP_l(\cos(\theta))\right], \tag{6}$$

or

$$\begin{aligned} R_i(\theta) \;=\; R_i\Bigg[&1+\beta_2\sqrt{\frac{5}{4\pi}}\left(\frac{3}{2}\cos^2(\theta)-\frac{1}{2}\right) \\ &+\beta_4\sqrt{\frac{9}{4\pi}}\frac{1}{64}(9+20\cos(2\theta)+35\cos(4\theta)) \\ &+\beta_6\sqrt{\frac{13}{4\pi}}\frac{1}{16}(231\cos^6(\theta)-315\cos^4(\theta) \\ &+105\cos^2(\theta)-5)\Bigg]. \end{aligned} \tag{7}$$

where θ is the angle between the axis of symmetry of the parent or daughter and the alpha emission direction and P_l denotes the Legendre function. The deformation parameter $\beta_l=\beta_{l0}$ is determined via [26]

$$\beta_{lm}=\sqrt{4\pi}\frac{\int R_i(\theta,\varphi)Y_l^{m}(\theta,\varphi)\mathrm{d}\Omega}{\int R_i(\theta,\varphi)Y_0^{0}(\theta,\varphi)\mathrm{d}\Omega}, \tag{8}$$

where

$$Y_l^m(\theta,\varphi)=\sqrt{\frac{2l+1}{4\pi}}P_l(\cos(\theta))\mathrm{e}^{\mathrm{i}m\varphi}. \tag{9}$$

The proximity potential $V_{prox}(z)$ is considered as [24]

$$V_{prox}(z)=4\pi\gamma b\frac{C_dC_\alpha}{C_t}\Phi\left(\frac{z}{b}\right), \tag{10}$$

with the nuclear surface tension coefficient being

$$\gamma=0.9517\left[1-1.7826\frac{(N_p-Z_p)^2}{A_p^2}\right](\mathrm{MeV/fm^2}). \tag{11}$$

For the general proximity potential we normally consider [21]

$$\begin{cases} \Phi(\varepsilon) \;=\; -1.7817+0.9270\varepsilon+0.0169\varepsilon^2 \\ \qquad\quad -0.05148\varepsilon^3 \;\; 0\leqslant\varepsilon\leqslant1.9475, \\ \Phi(\varepsilon) \;=\; -4.41\mathrm{e}^{\frac{-\varepsilon}{0.7176}} \;\; \varepsilon\geqslant1.9475, \end{cases} \tag{12}$$

where $\varepsilon=\dfrac{z}{b}$. The constants a_0,a_1 and a_2 are determined from the continuity conditions of the potential and its derivative, i.e. [20]

$$\begin{cases} \text{(i)}V(R_P)=Q. \\ \text{(ii)}V(r)=V(C_t)\&V'(r)=V'(C_t). \end{cases} \tag{13}$$

On the other hand, according to the WKB approximation, the penetration probability is

$$P=\exp\left\{-\frac{2}{\hbar}\int_{R_a}^{R_b}\sqrt{2\mu(V(r)-Q)}\mathrm{d}r\right\}, \tag{14}$$

in which the decay energy Q is obtained via [27, 28]

$$Q = B(Z-2,A-4)+28.3-B(Z,A)(\mathrm{MeV}), \quad (15)$$

$$B(Z,A) = 7.298Z+8.071(A-Z)-M(A,Z)(\mathrm{MeV}), \quad (16)$$

where $B(A,Z)$ and $M(A,Z)$ respectively denote the binding energy and the excess mass. The turning boundaries are obtained via $V_{\mathrm{Eq.(1)}}(r)=Q$. This equation has two roots; $r_1=R_{\mathrm{p}}$ and $r_2=R_{\mathrm{in}}=R_{\mathrm{a}}$ with $r_2\geqslant r_1$ and $V(R_{\mathrm{out}}=R_{\mathrm{b}})=Q$. We have plotted the potential in Fig. 1. The HL is obtained via [29]

$$T_{1/2}=\frac{\ln 2}{\lambda}=\frac{\ln 2}{\nu P}(\mathrm{s}), \quad (17)$$

Table 1. Alpha decay half-lives for ground state to ground state transition.

decay modes	I_{i}^{π}	I_{f}^{π}	parent deformation β_2	parent deformation β_4	parent deformation β_6	daughter deformation β_2	daughter deformation β_4	$T_{1/2}^{\mathrm{cal}}$/s	$T_{1/2}^{\mathrm{cal}}$/s Ref. [29]	$T_{1/2}^{\mathrm{exp}}$/s
^{152}Ho→^{148}Tb	2^-	2^-	0	0	0	0	0	1.684×10^{3}	2.35×10^{3}	1.35×10^{3}
			0	0	0	−0.052	0.009	1.682×10^{3}		
			0.126	0.038	0.016	0	0	1.684×10^{3}		
			0.126	0.038	0.016	−0.052	0.009	1.682×10^{3}		
^{154}Ho→^{150}Tb	2^-	2^-	0	0	0	0	0	1.236×10^{6}	1.88×10^{6}	3.71×10^{6}
			0	0	0	0.143	0.048	1.225×10^{6}		
			0.170	0.044	−0.001	0	0	1.236×10^{6}		
			0.170	0.044	−0.001	0.143	0.048	1.225×10^{6}		
^{156}Lu→^{152}Tm	2^-	2^-	0	0	0	0	0	8.255×10^{-1}	1.06	4.94×10^{-1}
			0	0	0	−0.052	0.009	8.247×10^{-1}		
			−0.104	0.012	0.003	0	0	8.255×10^{-1}		
			−0.104	0.012	0.003	−0.52	0.009	8.247×10^{-1}		
^{159}Ta→^{155}Lu	2^-	2^-	0	0	0	0	0	3.325	3.05	2.44
			0	0	0	0.035	0	3.324		
			0.107	0.012	0.005	0	0	3.325		
			0.107	0.012	0.005	0.035	0	3.324		
^{160}Ta→^{156}Lu	2^-	2^-	0	0	0	0	0	3.803×10^{1}	5.61×10^{1}	⩾1.7
			0	0	0	−0.104	0.012	3.788×10^{1}		
			0.134	0.022	0.005	0	0	3.803×10^{1}		
			0.134	0.022	0.005	−0.104	0.012	3.788×10^{1}		
^{153}Tm→^{149}Ho	$\frac{11^-}{2}$	$\frac{11^-}{2}$	0	0	0	0	0	3.123	3.74	1.63
			0	0	0	−0.008	0	3.123		
			−0.018	0	0	0	0	3.123		
			−0.018	0	0	−0.008	0	3.123		
^{156}Hf→^{152}Yb	0^+	0^+	0	0	0	0	0	3.894×10^{-2}	9.96×10^{-3}	2.34×10^{-2}
			0	0	0	0	0	3.894×10^{-2}		
			0.035	−0.008	0.001	0	0	3.894×10^{-2}		
			0.035	−0.008	0.001	0	0	3.894×10^{-2}		
^{158}W→^{154}Hf	0^+	0^+	0	0	0	0	0	2.350×10^{-3}	2.37×10^{-3}	1.37×10^{-3}
			0	0	0	0.008	0	2.350×10^{-3}		
			0.018	0	0.002	0	0	2.350×10^{-3}		
			0.018	0	0.002	0.008	0	2.350×10^{-3}		
^{163}Re→^{159}Ta	$\frac{1}{2}^+$	$\frac{1}{2}^+$	0	0	0	0	0	1.035	1.54	1.22
			0	0	0	0.107	0.012	1.035		
			0.125	0.006	0.001	0	0	1.039		
			0.125	0.006	0.001	0.107	0.012	1.035		
^{165}Re→^{161}Ta	$\frac{1}{2}^+$	$\frac{1}{2}^+$	0	0	0	0	0	3.860×10^{1}	7.71×10^{1}	5.22×10^{1}
			0	0	0	0.143	0.016	3.833×10^{1}		
			0.153	0	−0.002	0	0	3.860×10^{1}		
			0.153	0	−0.002	0.143	0.016	3.833×10^{1}		

Table 1 (continued)

decay modes	I_i^π	I_f^π	parent deformation			daughter deformation		$T_{1/2}^{cal}$/s	$T_{1/2}^{cal}$/s Ref. [29]	$T_{1/2}^{exp}$/s
			β_2	β_4	β_6	β_2	β_4			
$^{166}Ir \to ^{162}Re$	2^-	2^-	0	0	0	0	0	1.577×10^{-2}	2.10×10^{-2}	1.13×10^{-2}
			0	0	0	0.116	0.013	1.570×10^{-2}		
			0.107	−0.004	0.004	0	0	1.578×10^{-2}		
			0.107	−0.004	0.004	0.116	0.013	1.570×10^{-2}		
$^{167}Ir \to ^{163}Re$	$\frac{1}{2}^+$	$\frac{1}{2}^+$	0	0	0	0	0	9.211×10^{-2}	1.37×10^{-1}	7.19×10^{-2}
			0	0	0	0.125	0.006	9.164×10^{-2}		
			0.116	−0.011	0.002	0	0	9.211×10^{-2}		
			0.116	−0.011	0.002	0.125	0.006	9.164×10^{-2}		
$^{169}Ir \to ^{165}Re$	$\frac{1}{2}^+$	$\frac{1}{2}^+$	0	0	0	0	0	2.096	3.75	8.40×10^{-1}
			0	0	0	0.153	0	2.080		
			0.134	−0.009	−0.001	0	0	2.096		
			0.134	−0.009	−0.001	0.153	0	2.080		
$^{172}Pt \to ^{168}Os$	0^+	0^+	0	0	0	0	0	2.982×10^{-1}	4.26×10^{-1}	1.03×10^{-1}
			0	0	0	0.162	−0.006	2.956×10^{-1}		
			0.126	−0.010	−0.002	0	0	2.982×10^{-1}		
			0.126	−0.010	−0.002	0.162	−0.006	2.956×10^{-1}		
$^{170}Au \to ^{166}Ir$	2^-	2^-	0	0	0	0	0	2.600×10^{-3}	3.77×10^{-3}	2.00×10^{-3}
			0	0	0	0.107	−0.004	2.590×10^{-3}		
			−0.096	−0.012	−0.002	0	0	2.600×10^{-3}		
			−0.096	−0.012	−0.002	0.107	−0.004	2.590×10^{-3}		
$^{173}Au \to ^{169}Ir$	$\frac{1}{2}^+$	$\frac{1}{2}^+$	0	0	0	0	0	3.380×10^{-2}	5.43×10^{-2}	2.07×10^{-2}
			0	0	0	0.134	−0.009	3.360×10^{-2}		
			−0.105	−0.011	0.001	0	0	3.380×10^{-2}		
			−0.105	−0.011	0.001	0.134	−0.009	3.360×10^{-2}		
$^{177}Au \to ^{173}Ir$	$\left(\frac{1}{2},\frac{3}{2}\right)^+$	$\left(\frac{3}{2},\frac{5}{2}\right)^+$	0	0	0	0	0	7.681	5.35	3.66
			0	0	0	0.162	−0.023	7.600		
			−0.130	−0.009	0	0	0	7.681		
			−0.130	−0.009	0	0.162	−0.023	7.600		
$^{176}Hg \to ^{172}Pt$	0^+	0^+	0	0	0	0	0	5.075×10^{-2}	6.72×10^{-2}	2.10×10^{-2}
			0	0	0	0.126	−0.010	5.047×10^{-2}		
			−0.105	−0.027	0	0	0	5.075×10^{-2}		
			−0.105	−0.027	0	0.126	−0.010	5.047×10^{-2}		
$^{177}Tl \to ^{173}Au$	$\frac{1}{2}^+$	$\frac{1}{2}^+$	0	0	0	0	0	3.457×10^{-2}	5.53×10^{-2}	2.47×10^{-2}
			0	0	0	−0.105	−0.011	3.443×10^{-2}		
			−0.053	−0.007	0	0	0	3.457×10^{-2}		
			−0.053	−0.007	0	−0.105	−0.011	3.443×10^{-2}		
$^{179}Tl \to ^{175}Au$	$\frac{1}{2}^+$	$\frac{1}{2}^+$	0	0	0	0	0	6.268×10^{-1}	1.03	2.30×10^{-1}
			0	0	0	−0.122	−0.010	6.233×10^{-1}		
			−0.053	−0.007	0	0	0	6.268×10^{-1}		
			−0.053	−0.007	0	−0.122	−0.010	6.233×10^{-1}		
$^{181}Tl \to ^{177}Au$	$\frac{1}{2}^+$	$\left(\frac{1}{2},\frac{3}{2}\right)^+$	0	0	0	0	0	4.995×10^{1}	4.01×10^{1}	$>3.20\times10^{1}$
			0	0	0	−0.130	−0.009	4.959×10^{1}		
			−0.053	−0.007	0	0	0	4.995×10^{1}		
			−0.053	−0.007	0	−0.130	−0.009	4.959×10^{1}		
$^{180}Pb \to ^{176}Hg$	0^+	0^+	0	0	0	0	0	5.214×10^{-3}	7.84×10^{-3}	4.00×10^{-3}
			0	0	0	−0.105	−0.027	5.187×10^{-3}		
			0.008	−0.008	0.003	0	0	5.214×10^{-3}		
			0.008	−0.008	0.003	−0.105	−0.027	5.187×10^{-3}		

Table 1 (continued)

decay modes	I_i^π	I_f^π	parent deformation			daughter deformation		$T_{1/2}^{cal}$/s	$T_{1/2}^{cal}$/s Ref. [29]	$T_{1/2}^{exp}$/s
			β_2	β_4	β_6	β_2	β_4			
$^{188}Po \rightarrow ^{184}Pb$	0^+	0^+	0	0	0	0	0	1.882×10^{-4}	2.74×10^{-4}	2.70×10^{-4}
			0	0	0	0.009	−0.008	1.882×10^{-4}		
			0.293	0.007	−0.010	0	0	1.882×10^{-4}		
			0.293	0.007	−0.010	0.009	−0.008	1.882×10^{-4}		
$^{192}Po \rightarrow ^{188}Pb$	0^+	0^+	0	0	0	0	0	4.701×10^{-2}	7.90×10^{-2}	3.23×10^{-2}
			0	0	0	0	−0.008	4.700×10^{-2}		
			−0.207	0.008	0.001	0	0	4.701×10^{-2}		
			−0.207	0.008	0.001	0	−0.008	4.700×10^{-2}		
$^{193}Po \rightarrow ^{189}Pb$	$\frac{3}{2}^-$	$\frac{3}{2}^-$	0	0	0	0	0	2.886×10^{-1}	5.04×10^{-1}	4.20×10^{-1}
			0	0	0	0	−0.008	2.886×10^{-1}		
			−0.215	0.009	0.002	0	0	2.886×10^{-1}		
			−0.215	0.009	0.002	0	−0.008	2.886×10^{-1}		
$^{197}Po \rightarrow ^{193}Pb$	$\frac{3}{2}^-$	$\frac{3}{2}^-$	0	0	0	0	0	1.399×10^{2}	2.34×10^{2}	1.27×10^{2}
			0	0	0	0	−0.015	1.398×10^{2}		
			0.062	0.001	−0.002	0	0	1.399×10^{2}		
			0.062	0.001	−0.002	0	−0.015	1.398×10^{2}		
$^{199}Po \rightarrow ^{195}Pb$	$\frac{3}{2}^-$	$\frac{3}{2}^-$	0	0	0	0	0	4.032×10^{3}	6.56×10^{3}	2.74×10^{3}
			0	0	0	0.009	−0.015	4.030×10^{3}		
			0	−0.015	0	0	0	4.032×10^{3}		
			0	−0.015	0	0.009	−0.015	4.030×10^{3}		
$^{201}Po \rightarrow ^{197}Pb$	$\frac{3}{2}^-$	$\frac{3}{2}^-$	0	0	0	0	0	8.150×10^{4}	1.65×10^{5}	5.74×10^{4}
			0	0	0	0	−0.008	8.149×10^{4}		
			0	−0.015	0	0	0	8.150×10^{4}		
			0	−0.015	0	0	−0.008	8.149×10^{4}		
$^{198}At \rightarrow ^{194}Bi$	3^+	3^+	0	0	0	0	0	3.901	7.26	4.67
			0	0	0	−0.052	0.009	3.897		
			−0.207	−0.007	−0.001	0	0	3.901		
			−0.207	−0.007	−0.001	−0.052	0.009	3.897		
$^{200}At \rightarrow ^{196}Bi$	3^+	3^+	0	0	0	0	0	5.854×10^{1}	1.08×10^{2}	8.27×10^{1}
			0	0	0	0.052	0.009	5.847×10^{1}		
			0.089	−0.006	−0.001	0	0	5.854×10^{1}		
								5.847×10^{1}		
$^{202}At \rightarrow ^{198}Bi$	$(2,3)^+$	$(2,3)^+$	0	0	0	0	0	6.053×10^{2}	1.16×10^{3}	4.97×10^{2}
			0	0	0	0.009	−0.052	6.029×10^{2}		
			0.062	−0.007	0.001	0	0	6.053×10^{2}		
			0.062	−0.007	0.001	0.009	−0.052	6.029×10^{2}		
$^{195}Rn \rightarrow ^{191}Po$	$\frac{3}{2}^-$	$\frac{3}{2}^-$	0	0	0	0	0	1.590×10^{-2}	2.81×10^{-2}	6.00×10^{-3}
			0	0	0	0.275	−0.031	1.548×10^{-2}		
			−0.24	0.013	0.003	0	0	1.590×10^{-2}		
			−0.24	0.013	0.003	0.275	−0.031	1.548×10^{-2}		
$^{197}Rn \rightarrow ^{193}Po$	$\frac{3}{2}^-$	$\frac{3}{2}^-$	0	0	0	0	0	1.373×10^{-1}	2.54×10^{-1}	6.50×10^{-2}
			0	0	0	−0.215	0.009	1.350×10^{-1}		
			−0.232	0.012	0.002	0	0	1.373×10^{-1}		
			−0.232	0.012	0.002	−0.215	0.009	1.350×10^{-1}		
$^{199}Rn \rightarrow ^{195}Po$	$\frac{3}{2}^-$	$\frac{3}{2}^-$	0	0	0	0	0	1.443	5.30×10^{-1}	6.60×10^{-1}
			0	0	0	0.071	0.002	1.440		
			−0.207	0.001	−0.001	0	0	1.443		
			−0.207	0.001	−0.001	0.071	0.002	1.440		

Table 1 (continued)

decay modes	I_i^π	I_f^π	parent deformation			daughter deformation		$T_{1/2}^{cal}$/s	$T_{1/2}^{cal}$/s Ref. [29]	$T_{1/2}^{exp}$/s
			β_2	β_4	β_6	β_2	β_4			
^{201}Rn→^{197}Po	$\frac{3}{2}^-$	$\frac{3}{2}^-$	0	0	0	0	0	1.354×10^1	2.63×10^1	1.37×10^1
			0	0	0	0.062	0.001	1.352×10^1		
			−0.199	−0.016	−0.001	0	0	1.354×10^1		
			−0.199	−0.016	−0.001	0.062	0.001	1.352×10^1		
^{203}Rn→^{199}Po	$\frac{3}{2}^-$	$\frac{3}{2}^-$	0	0	0	0	0	1.149×10^2	2.21×10^2	6.67×10^1
			0	0	0	0	−0.015	1.149×10^2		
			−0.104	0.004	0.004	0	0	1.149×10^2		
			−0.104	0.004	0.004	0	−0.015	1.149×10^2		
^{201}Fr→^{197}At	$\frac{9}{2}^-$	$\frac{9}{2}^-$	0	0	0	0	0	1.419×10^{-1}	2.46×10^{-1}	6.20×10^{-2}
			0	0	0	−0.207	0.001	1.396×10^{-1}		
			−0.215	−0.006	0.001	0	0	1.419×10^{-1}		
			−0.215	−0.006	0.001	−0.207	0.001	1.396×10^{-1}		
^{202}Fr→^{198}At	3^+	3^+	0	0	0	0	0	3.949×10^{-1}	7.07×10^{-1}	3.00×10^{-1}
			0	0	0	−0.207	−0.007	3.884×10^{-1}		
			−0.207	−0.015	0.001	0	0	3.949×10^{-1}		
			−0.207	−0.015	0.001	−0.207	−0.007	3.884×10^{-1}		
^{203}Fr→^{199}At	$\frac{9}{2}^-$	$\frac{9}{2}^-$	0	0	0	0	0	1.124	3.25×10^{-1}	5.79×10^{-1}
			0	0	0	0.08	0.002	1.121		
			−0.190	−0.018	0.003	0	0	1.121		
			−0.190	−0.018	0.003	0.080	0.002	1.121		
^{204}Fr→^{200}At	3^+	3^+	0	0	0	0	0	2.234	0.79	1.77
			0	0	0	0.089	−0.006	2.234		
			−0.190	−0.024	0	0	0	2.241		
			−0.190	−0.024	0	0.089	−0.006	2.234		
^{206}Fr→^{202}At	$(2,3)^+$	$(2,3)^+$	0	0	0	0	0	1.906×10^1	1.25×10^1	1.90×10^1
			0	0	0	0.062	−0.007	1.903×10^1		
			−0.013	0.005	0.006	0	0	1.906×10^1		
			−0.013	0.005	0.006	0.062	−0.007	1.903×10^1		
^{203}Ra→^{199}Rn	$\frac{3}{2}^-$	$\frac{3}{2}^-$	0	0	0	0	0	6.234×10^{-2}	1.05×10^{-1}	3.10×10^{-2}
			0	0	0	−0.207	0.001	6.134×10^{-2}		
			−0.207	−0.015	0.001	0	0	6.234×10^{-2}		
			−0.207	−0.015	0.001	−0.207	0.001	6.134×10^{-2}		
^{205}Ra→^{201}Rn	$\frac{3}{2}^-$	$\frac{3}{2}^-$	0	0	0	0	0	4.277×10^{-1}	7.80×10^{-1}	$\geqslant2.10\times10^{-1}$
			0	0	0	−0.199	−0.016	4.208×10^{-1}		
			−0.190	−0.024	0.003	0	0	4.277×10^{-1}		
			−0.190	−0.024	0.003	−0.199	−0.016	4.208×10^{-1}		
^{207}Ra→^{203}Rn	$\left(\frac{5}{2},\frac{3}{2}\right)^-$	$\left(\frac{5}{2},\frac{3}{2}\right)^-$	0	0	0	0	0	2.316	2.81	1.44
			0	0	0	−0.104	0.004	2.306		
			−0.130	−0.002	0.007	0	0	2.316		
			−0.130	−0.002	0.007	−0.104	0.004	2.306		
^{206}Ac→^{202}Fr	3^+	3^+	0	0	0	0	0	2.914×10^{-2}	5.24×10^{-2}	2.20×10^{-2}
			0	0	0	−0.207	−0.015	2.865×10^{-2}		
			−0.207	−0.030	0.003	0	0	2.914×10^{-2}		
			−0.207	−0.030	0.003	−0.207	−0.015	2.865×10^{-2}		
^{208}Ac→^{204}Fr	3^+	3^+	0	0	0	0	0	1.461×10^{-1}	2.63×10^{-1}	9.60×10^{-2}
			0	0	0	−0.190	−0.024	1.438×10^{-1}		
			−0.190	−0.024	0.006	0	0	1.461×10^{-1}		
			−0.190	−0.024	0.006	−0.190	−0.024	1.438×10^{-1}		

Table 1 (continued)

decay modes	I_i^π	I_f^π	parent deformation β_2	β_4	β_6	daughter deformation β_2	β_4	$T_{1/2}^{cal}$/s	$T_{1/2}^{cal}$/s Ref. [29]	$T_{1/2}^{exp}$/s
$^{217}Pa \rightarrow ^{213}Ac$	$\frac{9}{2}^-$	$\frac{9}{2}^-$	0	0	0	0	0	2.163×10^{-3}	3.93×10^{-3}	3.48×10^{-3}
			0	0	0	−0.044	−0.015	2.161×10^{-3}		
			0	0.008	0	0	0	2.163×10^{-3}		
			0	0.008	0	−0.044	−0.015	2.161×10^{-3}		
$^{174}Ir \rightarrow ^{170}Re$	3^+	5^+	0	0	0	0	0	8.456×10^{2}	1.02×10^{2}	1.58×10^{2}
			0	0	0	0.199	−0.019	8.326×10^{2}		
			0.171	−0.022	−0.001	0	0	8.456×10^{2}		
			0.171	−0.022	−0.001	0.199	−0.019	8.326×10^{2}		
$^{183}Pb \rightarrow ^{179}Hg$	$\frac{3}{2}^-$	$\frac{7}{2}^-$	0	0	0	0	0	5.234×10^{-1}	6.27×10^{-1}	8.11×10^{-1}
			0	0	0	−0.122	−0.018	5.200×10^{-1}		
			0.009	0.015	0.004	0	0	5.234×10^{-1}		
			0.009	0.015	0.004	−0.122	−0.018	5.200×10^{-1}		
$^{185}Pb \rightarrow ^{181}Hg$	$\frac{3}{2}^-$	$\frac{1}{2}^-$	0	0	0	0	0	3.723	4.55	3.15×10^{3}
			0	0	0	−0.122	−0.018	3.698		
			0.009	0.015	0.002	0	0	3.723		
			0.009	0.015	0.002	−0.122	−0.018	3.698		
$^{187}Pb \rightarrow ^{183}Hg$	$\frac{3}{2}^-$	$\frac{1}{2}^-$	0	0	0	0	0	5.736×10^{1}	7.15×10^{1}	2.17×10^{2}
			0	0	0	−0.130	−0.017	5.692×10^{1}		
			0	−0.015	0.001	0	0	5.736×10^{1}		
			0	−0.015	0.001	−0.130	−0.017	5.692×10^{1}		
$^{186}Bi \rightarrow ^{182}Tl$	3^+	2^-	0	0	0	0	0	1.026×10^{-3}	1.37×10^{-3}	1.48×10^{-2}
			0	0	0	−0.053	−0.007	1.025×10^{-3}		
			−0.052	0.016	−0.001	0	0	1.026×10^{-3}		
			−0.052	0.016	−0.001	−0.053	−0.007	1.025×10^{-3}		
$^{191}Bi \rightarrow ^{187}Tl$	$\frac{9}{2}^-$	$\frac{1}{2}^+$	0	0	0	0	0	8.978×10^{1}	2.69×10^{1}	2.05×10^{1}
			0	0	0	−0.053	−0.007	8.969×10^{1}		
			−0.052	0.009	0	0	0	8.978×10^{1}		
			−0.052	0.009	0	−0.053	−0.007	8.969×10^{1}		
$^{193}Bi \rightarrow ^{189}Tl$	$\frac{9}{2}^-$	$\frac{1}{2}^+$	0	0	0	0	0	7.456×10^{3}	2.30×10^{3}	1.91×10^{3}
			0	0	0	−0.053	−0.007	7.449×10^{3}		
			−0.052	0.009	0	0	0	7.456×10^{3}		
			−0.052	0.009	0	−0.053	−0.007	7.449×10^{3}		
$^{194}Bi \rightarrow ^{190}Tl$	3^+	2^-	0	0	0	0	0	1.156×10^{4}	1.91×10^{4}	2.05×10^{4}
			0	0	0	−0.061	−0.007	1.154×10^{4}		
			−0.052	0.009	0	0	0	1.156×10^{4}		
			−0.052	0.009	0	−0.061	−0.007	1.154×10^{4}		
$^{195}Bi \rightarrow ^{191}Tl$	$\frac{9}{2}^-$	$\frac{1}{2}^+$	0	0	0	0	0	9.862×10^{5}	3.36×10^{5}	5.72×10^{5}
			0	0	0	−0.053	−0.007	9.854×10^{5}		
			−0.052	0.009	0	0	0	9.862×10^{5}		
			−0.052	0.009	0	−0.053	−0.007	9.854×10^{5}		
$^{216}Ac \rightarrow ^{212}Fr$	1^-	5^+	0	0	0	0	0	1.100×10^{-4}	3.32×10^{-5}	4.40×10^{-4}
			0	0	0	−0.008	0.008	1.100×10^{-4}		
			−0.018	0.008	−0.003	0	0	1.100×10^{-4}		
			−0.018	0.008	−0.003	−0.008	0.008	1.100×10^{-4}		

where $\nu=(\omega/2\pi)=(2E/h)$ is the frequency of collision with barrier per second and λ is the decay constant. E is the empirical zero point vibration energy given by [30]

$$E=Q\left\{0.056+0.039\exp\left[\frac{(4-A_{\alpha})}{2.5}\right]\right\}(\text{MeV}). \tag{18}$$

Substitution of E and P in (17) determines the HL. The corresponding results are reported in Table 1.

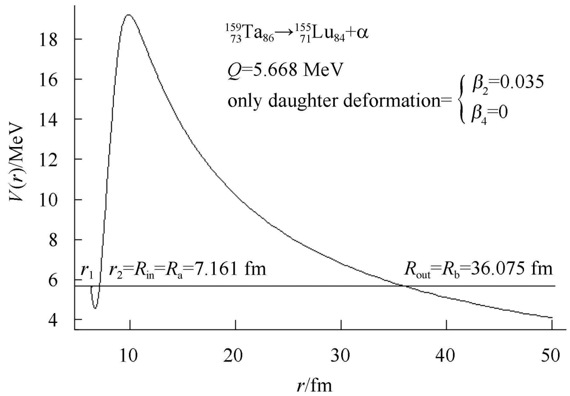

Fig. 1. The potential vs. the distance between the fragment centers ($R_{\rm a}$ and $R_{\rm b}$ being the first and second turning points, respectively).

3 Numerical results

As a typical example, the continuity conditions (i) and (ii) for ${}^{180}\text{Pb}\rightarrow{}^{176}\text{Hg}$ determined the potential give $a_0=284.691$, $a_1=-79.605$ and $a_2=5.696$. The experimental HL for this nucleus is $(4.00\times10^{-3}$ s). When we assume a spherical shape for Pb, the calculated HL is $(5.214\times10^{-3}$ s). For a deformed daughter with $\beta_2=-0.105$ and $\beta_4=-0.027$, the HL is $(5.178\times10^{-3}$ s). For a deformed parent, from the parameters $\beta_2=0.008$, $\beta_4=-0.008$ and $\beta_6=0.003$ obtained from the boundary conditions, the HL is $(5.214\times10^{-3}$ s). When we consider both the daughter and the parent of deformed shape, the HL is $(5.178\times10^{-3}$ s).

The Alpha emission obeys the spin-parity selection rule [29]:

$$|I_{\rm i}-I_{\rm f}|\leqslant l\leqslant I_{\rm i}+I_{\rm f} \quad \text{and} \quad \frac{\pi_{\rm i}}{\pi_{\rm f}}=(-1)^{l}, \tag{19}$$

where $I_{\rm i}$, $\pi_{\rm i}$ and $I_{\rm f}$, $\pi_{\rm f}$ are the spin and parity of the parent and daughter, respectively. We have calculated the HL of deformed nuclei in Gs to GS transitions and compared them with Ref. [29] in Table 1. The first column represents different modes of transition and, the fourth and the fifth columns are the deformation parameters of the parent and daughter, respectively. The seventh column shows our calculated HL. We see that the results are acceptable.

4 Conclusion

We consider an angle dependent-potential for the range $67\leqslant Z\leqslant91$. The dependence on angle leads to multiple approximations which are considered for three possible combinations, i.e., for the daughter, the parent and for both of them. It is revealed that the results are in closer agreement with the experimental data when the multiple approximation is considered only for the daughter.

References

1 Gamow G. Z. Phys., 1928, **51**: 204
2 Condon E U, Gurney R W. Nature (London), 1928, **122**: 439
3 XU C, REN Z. Nucl. Phys. A, 2005, **753**: 174
4 Ni D, REN Z. Nucl. Phys. A, 2009, **825**: 145
5 Royer G. Nucl. Phys. A, 2010, **848**: 279
6 Yibin Q, REN Z. Nucl. Phys. A, 2011, **852**: 82
7 Stone N J et al. Nucl. Phys. A, 2007, **793**: 1
8 Yibin Q et al. J. Phys. G: Particle and Nucl. Phys., 2011, **38**: 015102
9 Royer G, Zbiri K, Bonilla C. Nucl. Phys. A, 2004, **730**: 22
10 Tavares O A P, Medeiros E L, Terranova M L. J. Phys. G, 2005, **31**(2): 129
11 Medeiros E L, Rodriques M M B, Duarte S B, Tavares O A P. J. Phys. G, 2006, **32**(8): B23
12 REN Z, XU C. Nucl. Phys. A, 2005, **759**: 64
13 Samanta C, Chowdhury P R, Basu D N. Nucl. Phys. A, 2007, **789**(1–4): 142
14 Santhosh K P et al. Nucl. Phys. A, 2010, **832**(3–4): 220
15 Dasgupta-Schuber N, Reyes M A, Tamez V A. Eur. Phys. J. A, 2009, **42**(1): 121
16 Jeppesenet H B et al. Euro. Phys. J. A, 2007, **32**(1): 31
17 Raiola F et al. Euro. Phys. J. A, 2007, **32**(1): 51
18 XU C, REN Z. Phys. Rev. C, 2006, **73**: 041301
19 Denisov V Y, Ikezoe H. Phys. Rev. C, 2005, **72**: 064613
20 HU Z et al. Commun. Theor. Phys., 2011, **55**: 307
21 Blocki J, Swiatecki W J. Ann. Phys. (N.Y.), 1981, **132**: 53
22 Santhosh K P, Joseph A. Pram. J. Phys., 2002, **59**: 679
23 Shi Y J, Swiatecki W J. Nucle. Phys. A, 1987, **464**: 205
24 Blocki J, Randrup J, Swiatecki W J, Tsang C F. Ann. Phys. (N.Y.), 1977, **105**: 427
25 Krappe H J, Nix J R, Sierk A J. Phys. Rev. C, 1979, **20**: 992
26 Moller P, Nix J R, Myers W D, Swiatecki W J. At. Data Nucle. Data Tables, 1995, **59**: 185
27 Duflo J, Zuker A P. Phys. Rev. C, 1995, **52**: R23
28 Koura H, Tachibana T et al. Prog. Theor. Phys., 2005, **113**: 305
29 Santhosh K P, Joseph J G, Sahadevan S. Phys. Rev. C, 2010, **82**: 064605
30 Poenaru D N, Ivascu M, Sandulescu A, Greiner W. Phys. Rev. C, 1985, **32**: 572